

# Near Sun Free-Space Optical Communications from Space

A. Biswas<sup>1</sup>, F. Khatri<sup>2</sup>, D. Boroson<sup>2</sup>

<sup>1</sup>California Institute of Technology, Jet Propulsion Laboratory  
4800 Oak Grove Drive, Pasadena, CA 91109.

<sup>2</sup>MIT, Lincoln Laboratory, 244 Wood Street, Lexington, MA 02420

818-354-2415  
abiswas@jpl.nasa.gov

*Abstract*— Free-space optical communications offers expanded data return capacity, from probes distributed throughout the solar system and beyond. Space-borne and Earth-based optical transceivers used for communicating optically, will periodically encounter near Sun pointing. This will result in an increase in the scattered background-light flux, often contributing to degraded link performance. The varying duration of near Sun pointing link operations relative to the location of space-probes, is discussed in this paper. The impact of near Sun pointing on link performance for a direct detection photon-counting communications system is analyzed for both ground- and space-based Earth receivers. Finally, impact of near Sun pointing on space-borne optical transceivers is discussed.

**Keywords:** Free-space; laser communication; Sun-Earth Probe (SEP) angle; Sun-Probe-Earth (SPE) Angle.

## TABLE OF CONTENTS

1. INTRODUCTION .....	1
2. SUN ANGLES FROM EARTH AND SPACE .....	2
3. RECEIVED BACKGROUND AND SUN ANGLE.....	3
4. DOWNLINK OPTICAL COMM PERFORMANCE.....	5
5. SPACEBORNE OPTICAL TRANSCEIVERS.....	5
6. CONCLUSIONS .....	6
REFERENCES.....	6

## 1. INTRODUCTION

Future space exploration requires expanded communications capacity, in order to facilitate the use of higher resolution science instruments. Optical communications, based upon transmitting near diffraction limited laser beams from space, is an emerging technology that can greatly augment and enhance the required communications capacity.

However, in order to realize the full potential of free-space optical communications, critical demonstrations are needed in order to advance the technology into a reliable and robust operational capability. With this in mind NASA had recently initiated the Mars Laser Communication Demonstration (MLCD) Project<sup>1</sup> managed by the Goddard Space Flight Center (GSFC). An optical transceiver developed by MIT, Lincoln

Laboratories (LL) known as the Mars Laser Terminal (MLT) was to fly aboard the Mars Telecom Orbiter (MTO), managed by the California Institute of Technology, Jet Propulsion Laboratory (JPL). Science and telemetry data was to be down-linked optically to two receive terminals, namely, the Palomar Receive Terminal<sup>2,3,4</sup> (PRT), developed by JPL, based upon modification of the Hale telescope at Palomar Mountain and the Link Development and Evaluation System<sup>5</sup> Receive Terminal (LDES RT), developed by MIT/LL to be located in Arizona. Separate transmit terminals (TT) were to be used for transmitting lasers to MLT. These were the Optical Communications Telescope Laboratory transmit terminal (OCTL TT) developed by JPL and located at the NASA/JPL Table Mountain Facility near Wrightwood, CA and a separate LDES aperture co-located with the receive terminal. Subsequently, NASA cancelled MTO resulting in the termination of the MLCD Project. However, successful system requirements and preliminary design reviews were completed. These requirements and design efforts addressed many critical issues related to free-space optical communications from deep-space, among which near-Sun pointing, that proved to be a design driver for the MLT and the ground-based receive and transmit terminals. In this paper the considerations and impacts of near Sun-pointing are presented in broader context, using and extending analytical techniques developed for the MLCD Project.

A summary of the near Sun-pointing durations expressed as a function of the synodic period for several solar system targets is summarized. The nature of the link degradation as a function of near Sun pointing for Earth-based receivers located on the ground and space are described with spaceprobe in Mars orbit as an example. Finally, the impact of near Sun pointing from remote optical transceivers is discussed.

## 2. SUN ANGLES FROM EARTH AND SPACE

Figure 1 shows a general view of the Sun-angle problem as it relates to free-space optical communications with the planet Mars, used as an example. When the line-of-sight (LOS) from an Earth-based receiver to a space probe is near the Sun, as quantified by a small SEP angle, a near Sun pointing situation is encountered. Under these conditions a spacecraft at Mars “looking” back at an Earth receiver will have the Sun close to its line-of-sight as characterized by the SPE angle. One difference for the

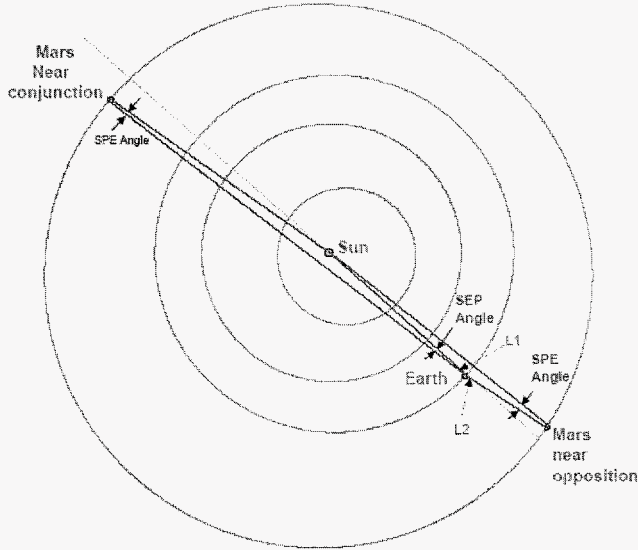


Figure 1 Relative position of Earth and Mars during small SEP and SPE angles

space-borne optical transceiver is that small SPE angles are encountered both during the conjunction and opposition of the outer planets, as shown in Figure 1, for planet Mars.

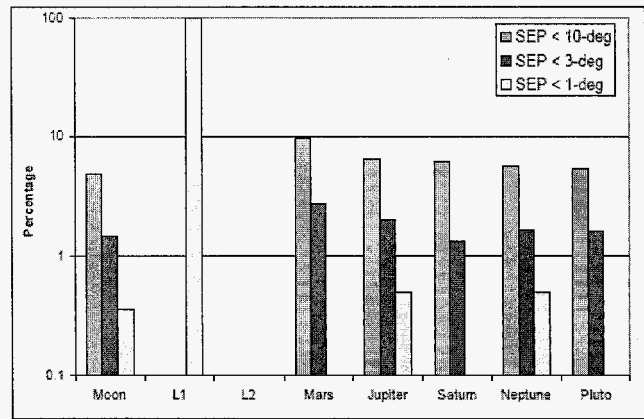
The duration of the near-Sun encounters is summarized in Figure 2 for a number of space missions of interest. Instead of using spacecraft orbital predicts the ephemerides of planets, the moon and dynamic Lagrange points, were used to determine SEP and SPE angles over a synodic period<sup>6</sup>. The percentage duration with SEP angles less than 10-, 3- and 1-degree(s) are shown in Figure 2a, while SPE angles less than 10, 2 and 1 are shown in Figure 1b. The percentages are estimated over a synodic period, that for Mars is approximately two years, while for all other outer planets is approximately 1 year. The absence of bars indicates that SEP or SPE angles less than the quantities in the legend are never encountered. The percentages are estimated on the total time that the planet or dynamic planet or satellite of interest is at > 10-degree elevation angle over Palomar Mountain, CA.

Figure 2 shows that for lunar missions, with a period of 1-month, the percentage average duration per year with SEP and SPE angles < 10-degrees is about 5%. SEP angles

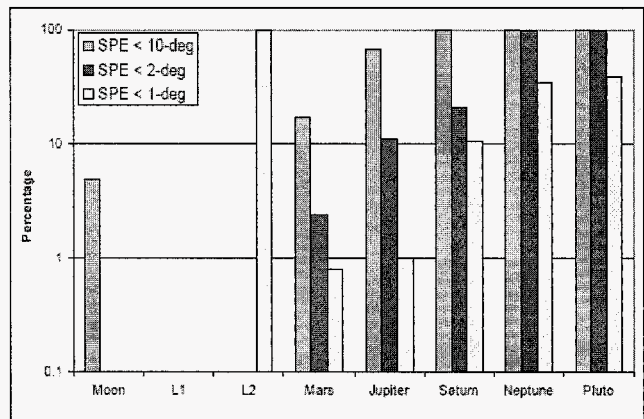
lower than 3- and 1-degrees are 1.5% and < 0.3%. On the other hand SPE angles lower than 2- and 1-degrees are < 0.1% of the time.

Optical links to and from the dynamic Lagrange points L1 and L2 (see Figure 1) present a somewhat unique combination of SEP and SPE angles. Earth-based receivers always have < 1-degree SEP angles for L1 missions while the SPE angles are never small. On the other hand for L2 missions the SPE angles are always < 1-degree while small SEP angles are never encountered.

For Mars and outer planets the fraction of time for small SEP angles are always < 10%. The percentage of duration at small SPE angles increases with range to the planet. Therefore significant outage durations will be encountered unless the space-borne optical transceiver can operate at very small SPE angles.



(a)



(b)

Figure 2 (a) The percentage of time spent at SEP angles less than 10- (blue), 3-(purple) and 1-degree (yellow). (b) The percentage of time spent at SPE angles less than 10- (blue), 3- (purple) and 1-degree (yellow).

Note that in systems design the specified SEP/SPE angle operational limits will imply outage durations and depending

upon the location of the Earth-based receiver, namely, ground or space, the outage percentage will contribute to the overall link availability. For example for a ground-based optical link a 90% weather availability<sup>7</sup> could be expected assuming a globally distributed network that accounts for weather diversity. So an additional 5-10% outage because the optical collector cannot be operated at Sun-elongation angles of < 3 or 10-degrees would result in an 80-85% overall link availability not accounting for times when the link may not be operable due to high winds combined with very poor atmospheric “seeing” even in the presence of cloud-free line of sight. Therefore trying to maintain operability close to the Sun becomes important.

Beyond Mars the fractional time at low SPE angles by far dominates near Sun operations and at Neptune and Pluto optical transceivers will have to be designed to operate at SPE angles less than 2-degrees.

The near Sun-pointing durations summarized in the figure above introduce an added element of “difficulty” for optical links. Traditionally<sup>8</sup>, the product of data rate and square of link range (Mbps-AU<sup>2</sup>) is used as an index of link difficulty, however, for optical links the proximity to the Sun and the resulting increase in background accompanying signal received at either end of the link adds to the difficulty. In order to quantify the effect of near-Sun pointing the location of the Earth-based or space borne optical transceiver must be taken into account. In the following sections some examples are provided.

### 3. RECEIVED BACKGROUND AND SUN ANGLE

For the Mars laser communication demonstration ground-based receivers were base-lined. Operating from the ground introduces link closure uncertainties due to blockage by clouds and varying amounts of link degradation due to the combined effects of atmospheric turbulence, sky brightness and atmospheric attenuation. On the other hand, the expense and development required for alternative optical collectors deployed above the Earth’s atmosphere, on high altitude airborne platforms or in space, is formidable and was deemed beyond the scope of the MLCD Project.

The background contributed by sky radiance  $\lambda_{sky-background}$  is given by:

$$\lambda_{sky-background} = L_{\lambda} \times A \times \Delta\lambda \times \Omega \quad (1)$$

where:

$L_{\lambda}$  = Sky radiance in (W/cm<sup>2</sup>/μm/sr)

A = Effective area of optical collector (cm<sup>2</sup>)

$\Delta\lambda$  = Optical bandpass (μm)

$\Omega$  = Solid angle (steradians)

With  $\Omega \approx \frac{\pi}{4} \theta_{FOV}^2$ , where  $\theta_{FOV}$  is the field-of-view.

$L_{\lambda}$  has a strong dependence upon the SEP angle<sup>9</sup> as shown in Figure 3. The colored lines are predicted sky radiance versus SEP angle along the principal plane using MODTRAN<sup>10</sup> for the indicated atmospheric models. The dots in Figure 3 are included to show how AERONET<sup>11</sup> measured data at Table Mountain, CA compares with the predictions. The atmospheric turbulence will determine the required angular extent of sky subtended on the detector, or FOV required to encircle a desired fraction of signal energy. The background will be proportional to the square of the required FOV. For a given FOV, however, lower SEP angles will always result in an increased “in-band” background contribution.

The planet that the spacecraft is orbiting, for example, Mars also reflects Sunlight and when it partially or fully overlaps the detector FOV, contributes to background. Though the amount of background from this source is also proportional to the square of  $\theta_{FOV}$ , it does not depend directly on the SEP angle.

Stray light, defined as the fraction of “in-band” background contributed by scattering from surface roughness and contamination, as a result of off-axis solar illumination of optical collector surface will also depend on proximity to the Sun. The stray light will depend upon the

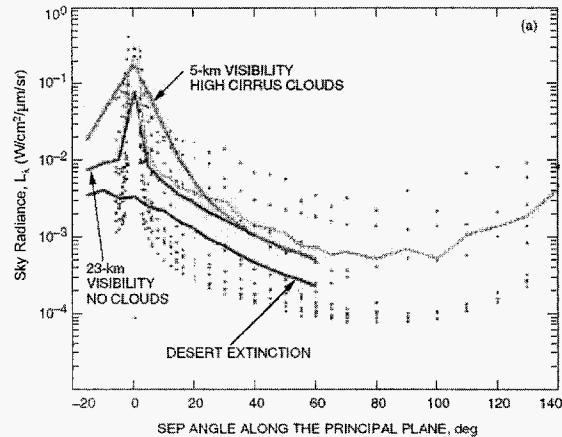


Figure 3 Comparison of MODTRAN predicted (colored lines) sky radiance with AERONET measurements (dots) at Table Mountain, CA

design of the optical collector. For the present discussion the Hale telescope at Palomar with a 5-m diameter collector and the point design used for MLCD, is used as an example.

In order to protect overheating of the primary mirror due to solar heating, as well as, protect telescope structural parts from re-focused light from the primary mirror a reflective solar rejection filter was used<sup>11</sup>. The filter covering the entrance aperture of the telescope was made up of a mosaic of filter panels as shown in the solid model rendition in Figure 4.

The bi-directional scatter distribution function (BSDF) for the solar rejection filter was modeled using two contributions, firstly,  $\rho_{fil}$ , from the micro-roughness, index inhomogeneities and scratch and dig and secondly,  $\rho_{con}$ , due surface contamination on the filter. The former was modeled for normal incidence with a scattering angle  $\theta$ , to be:

$$\rho_{fil}(\theta) = 0.1(100\sin\theta)^{-1.8} \quad (2)$$

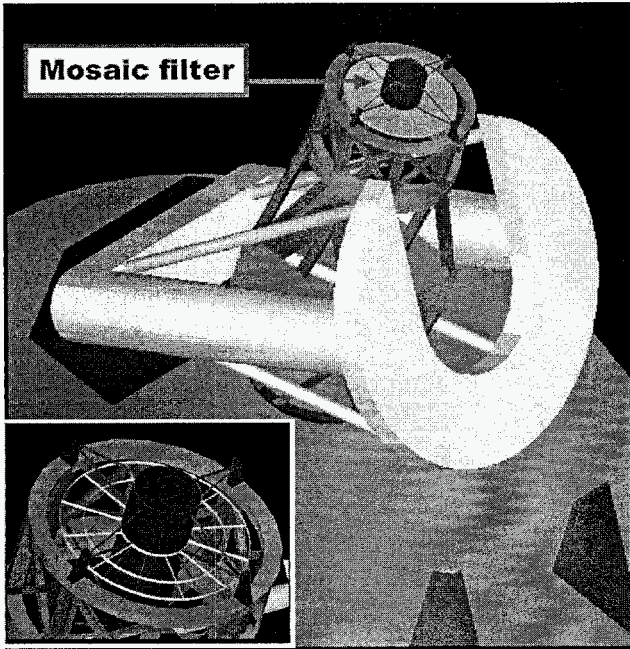


Figure 4 showing solar rejection filter mounted at entrance aperture of a solid model rendition of the Hale telescope. The inset shows the mosaic concept used for the scatter analysis.

while, the latter was modeled<sup>12</sup> as for a Level 500 cleanliness:

$$\rho_{con}(\theta) = 356 \left(1 + \frac{\sin^2\theta}{0.001^2}\right)^{-2.7} + 5.5 \times 10^{-4} \left(1 + \frac{\sin^2\theta}{0.1^2}\right)^{-0.5} \quad (3)$$

The stray light radiance as a function of angle is therefore given by:

$$L_{stray\_filter} = \eta_{atm} * Solar\_Const * (\rho_{fil} + \rho_{con}) \quad (4)$$

where,  $\eta_{atm}$  is the atmospheric transmission and the  $Solar\_Const$  is the irradiance per wavelength ( $W/cm^2/\mu m$ ) incident above the atmosphere at  $1.064\text{-}\mu m$ .

In the MLCD design the solar rejection filter transmitted 80% of the 1064-nm light. The fraction falling upon the primary mirror of the telescope can once again undergo scattering due to the micro-roughness and contamination on the primary mirror. The primary mirror bi-directional reflectance distribution function,  $\rho_{PM}$ , can be modeled as<sup>13</sup>

$$\rho_{PM}(\theta) = \left(\frac{s+2}{2\pi}\right) \times \left(\frac{4\pi\sigma}{\lambda}\right)^2 [\sin(\theta)]^s \quad (5)$$

where  $s = -1.8$ ,  $\sigma$  is the effective surface roughness which for the examples used in this discussion is assume to be 20 angstroms.  $\lambda$  is the operating wavelength. Again the scattered radiance from the primary mirror can be determined using Eqn. (5) and replacing solar filter BSDF with primary mirror BRDF and accounting for the transmission of the filter.

A summary of the background incident photon flux in photons/nanosecond upon the detector at the Cassegrain focus of the Hale telescope is shown in Figure 5.

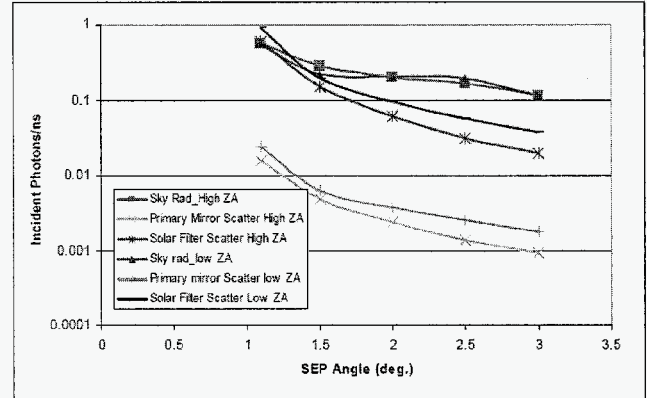


Figure 5 Background incident photon flux in photons/nanosecond from contributions that depend upon the SEP angle.

Note that in addition to the background contributions shown in Figure 4 there will be added background from Mars when it is in the detector field of view, however, this contribution does not depend upon SEP angle.

In Figure 5 a pair of data series, corresponding to high and low zenith angles, are shown for each scattered background category. During a spacecraft pass these two points correspond with when the spacecraft is rising above 10-degree elevation above Palomar Mountain, CA and the highest elevation angle for planet Mars during the 2010-2011 Mars-Earth solar conjunction. The diurnal and zenith

angle dependence of “seeing” and attenuation is accounted for in the background estimates shown<sup>14</sup>.

If the receiver were deployed sufficiently above the atmosphere or in space the atmospheric contributions, namely, sky radiance the increased field-of-view required to encircle a desired fraction of the signal energy would no longer apply. Scattering from the primary mirror would remain though contamination issues may be more benign in space. Whether a solar filter would be required by a space deployed receiver is a question beyond the scope of the present discussion. By the same token pointing and platform stabilization issues for a space based receiver and whether they incur additional link losses is also not addressed. Instead an upper bound on performance in space is provided assuming an effective primary surface roughness of 20-angstroms.

#### 4. DOWNLINK OPTICAL COMMUNICATIONS PERFORMANCE

Taking into account all the background contributions including the planet Mars in the field of view, the data-rate performance is summarized in Figure 6.

In deriving the data-rates in Figure 6 a 5-W average power transmitter with a 30-cm aperture diameter optical transceiver at Mars was assumed. The characteristics assumed for the transmitter are similar to the MLCD point design<sup>14,15</sup>.

Figure 6 shows a comparison of implementing similar sized apertures on the ground and in space. The atmospheric parameter variance contributes to the indicated error bars for the ground-based receiver performance. As mentioned earlier the performance loss as a function of decreasing SEP angle occurs at approximately the same range, introducing a new dimension to the data-rate and range squared product in describing link difficulty. The reason why the space deployed performance does not change with Sun-angle is that the field-of-view of the receiving optical detector is near diffraction limited so that the solid angle multiplier term (see equation 1) for determining background contribution is very small and the increase in scatter with Sun-angle does not have a measurable impact on performance given that the tool used estimates data rates in discrete steps.

Note that the ground and space-based performance will approach each other as the background decreases. The main difference under night sky conditions will be the relative contribution of background by the planet Mars.

Figure 6 also shows the link analysis results for a smaller 2.65-m diameter, optical collector deployed in space. The smaller diameter is closer to a practically deployable sized optical collector in space. Furthermore, a single performance point for a 10-m aperture with a solar rejection filter on the

ground is also shown. These data show provide an indication of the required aperture size on the ground that can come close to equaling performance of the upper bound of performance of a space-deployed receiver.

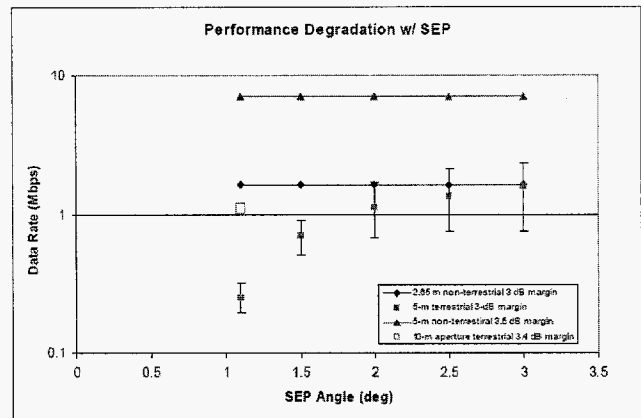


Figure 5 Optical communications performance near the Sun for Earth-based receivers with downlink from Mars using elements of the MLCD point design.

#### 5. SPACEBORNE OPTICAL TRANSCEIVERS

For the remote spaceborne optical transceivers, besides L2 missions where SPE angles are near zero all the time, longer durations of small SPE angles are encountered as missions extend farther in the solar system, as indicated in Figure 2b. Table 1 shows the SPE angle limit that the remote optical transceiver would have to be able to communicate from in order to operate the link 10% of the time.

TABLE 1

Year	Planet	Near Range (AU)	Far Range (AU)	SPE Angle (deg)
2010-2011	Mars	0.67	2.38	6
2009-2010	Jupiter	4.2	6.2	1.65
2009-2010	Saturn	8.4	10.4	0.95
2009-2010	Neptune	29	31	0.3
2016-2018	Pluto	32.2	34.2	0.275

MLT was designed to operate down to a 2-degree SPE angle indicating that SPE limitations would not restrict outages to 10%, however, from Jupiter on the SPE angles drop below 2-degrees. Table 1 also shows the near and far range to remind us that as mentioned, small SPE angles occur at the nearest and farthest ranges. The ephemerides used to arrive at the SPE angles were computed for the time-span shown in the first column of Table 1. A 10-degree elevation cut-off from Palomar Mountain was assumed for the ground-station.

Though stray light increases due to lower SPE angles will depend upon the design of the remote optical transceiver, for example, whether a solar rejection filter is used or not. Additionally there will be thermal design issues that are beyond the scope of the present discussion. Assuming the presence of a solar rejection filter and primary mirror equations 2, 3 and 5 can be used to estimate the increase in the BTDF of a filter maintained at Level 500 cleanliness and the BRDF of a primary mirror with an effectiveness surface roughness,  $\sigma$ , of 20 angstroms. Furthermore, since MLT design allowed operation at SPE = 2-degrees, the relative increase in scatter functions can be estimated. However, equation 4 shows that the solar-constant will drop as the inverse square of range. The latter term is by far dominant. Figure 6 shows the relative factors for increase in scatter, decrease in solar constant, resulting in nearly 2-orders of magnitude reduction in background, relative to the scatter at 0.7 AU at a an SPE degree of 2-degrees.

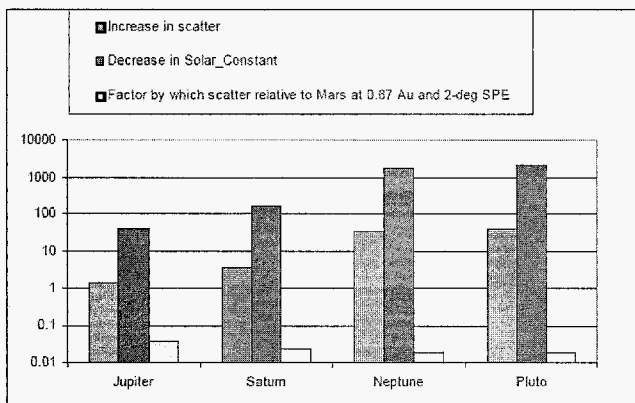


Figure 6 Comparison of scatter function and solar constant relative to and SPE angle of 2-degrees and a range of 0.67 AU.

The solar scatter into the remote optical transceivers focal plane will result in a degradation of the signal to noise received. The consequence of degraded SNR can impact pointing and uplink reception performance. From the simple analysis represented by Figure 6, Mars at closest range to Earth with a 2-degree SPE for which designs have been developed should be more than adequate for farther reaches of the solar system from stray light considerations.

## 6. CONCLUSIONS

The fractional durations of near Sun pointing from Earth receivers and remote optical transceivers were estimated for several missions of interest. The Lagrange point missions present a unique situation where either the receiver or transmitter has to continuously point close to the Sun. In order to keep near-Sun pointing outages from Earth-based receivers < 5% but > 1% designs that can tolerate SEP angles of 3-degrees are called for. Ground-based receivers are more severely impacted by near Sun

pointing due to the combined contributions from atmospheric and optical collector scatter, both of which are exacerbated by the increased FOV needed due to atmospheric turbulence. In order to recover loss in performance from a ground-based operations relative to above the atmosphere or space-based operations, approximately 5-times larger effective aperture diameters were needed for the MLCD link analysis example presented. The MLT design that was able to operate at SPE angles of 2-degrees, from the near Mars range indicates that outer planet mission will have no difficulty in pointing much closer to the Sun because of the inverse square decrease in solar constant.

## Acknowledgements

The authors would like to thank Gary Peterson of Breault Research Organization for contributions to the stray light estimation methods used. The work described was carried out jointly by the Jet Propulsion Laboratory, California Institute of Technology and the MIT, Lincoln Laboratories under contract with the National Aeronautics and Space Administration

## REFERENCES

- [1] S. A. Townes et al. "The Mars Laser Communication Demonstration," IEEE Aerospace Conference Proceedings, 1180, 2004
- [2] S. Franklin et al. "The 2009 Mars Telecom Orbiter Mission," IEEE Aerospace Conference Proceedings, 437, 2004
- [3] D. M. Boroson, A. Biswas, B. L. Edwards, "MLCD: Overview of NASA's Laser Communications Demonstration System," Proceedings of the SPIE, Free-Space Laser Communication Technologies XVI [ed. G. S. Mecherle, C. Y. Young, J. S. Stryjewski], 5338, 16, 2004.
- [4] D. M. Boroson, R. S. Bondurant, D. V. Murphy, "LDORA: a novel laser communications receiver array architecture," Proceedings of the SPIE, Free-Space Laser Communication Technologies XVI [ed. G. S. Mecherle, C. Y. Young, J. S. Stryjewski], 5338, 56, 2004.
- [5] K. Wilson, A. Vaughn, J. Wu, D. Mayes, J. Mahoney and R. Sobek, "Preliminary Characterization Results of the Optical Communications Telescope Laboratory Telescope," Inter-Planetary Network Progress Report, 42-161, 1-14, May 15, 2005
- [6] HORIZONS Ephemeris Generator

[7] R. Link, R. Alliss, M. E. Craddock, "Mitigating the impact of clouds on optical communications," Proceedings of the SPIE, Free-Space Laser Communication Technologies XVI [ed. G. S. Mecherle, C. Y. Young, J. S. Stryjewski], 5338, 223, 2004

[8] J. S. Schier, J. J. Rush, W. D. Williams, P. Vrotos, "Space Communications Supporting Exploration and Science: Plans and Studies for 2010-2030," 1<sup>st</sup> Space Exploration Conference: Continuing the Voyage of Discovery, AIAA 2005-2517.

[9] A. Biswas and S. Piazzolla, "Deep-Space Optical Communications Downlink Budget from Mars: System Parameters," Inter-Planetary Network Progress Report, 42-154, 1-38, August 15, 2003.

[10] A. Berk, L. S. Bernstein and D. C. Robertson, "MODTRAN: A Moderate Resolution Model for LOWTRAN 7," Airforce Geophysical Laboratory Technical Report GL-TR-89-0122, Hanscom AFB, MA.

[11] <http://aeronet.gsfc.nasa.gov>

[12] M. G. Dittman, "Contamination Scatter Functions from Stray Light Analysis," Proceedings of the SPIE, Optical System Contamination: Effects, Measurement and Control, 4774, 99-110, 2002.

[13] M. J. Britcliffe, D. J. Hoppe, W. Roberts and N. Page, "A ten-meter ground Station Telescope for Deep Space Optical Communications: A Preliminary Design," Inter-Planetary Network, Progress Report, 42-147, 1-17, November 15, 2001.

[14] F. I. Khatri, D. M. Boroson, D. V. Murphy, J. Sharma, "Link Analysis of Mars-Earth optical communications system," Proceedings of the SPIE, Free-Space Laser Communication Technologies XVI [ed. G. S. Mecherle, C. Y. Young, J. S. Stryjewski], 5338, 143, 2004.

[15] F. I. Khatri and A. Biswas, "Signal and Background Levels for the Mars Laser Communication Demonstration (MLCD)," IEEE LEOS Summer Topical Meeting – Free-Space Communication Techniques for Optical Networks.